



SIMULTANEOUS MEASUREMENTS OF PRESSURE AND DEFORMATION ON A UCAV IN THE SARL

Jim Crafton*, Sergey Fonov*, Edward G. Jones*, Larry Goss*, Charles Tyler**
***Innovative Scientific Solutions Inc., 2766 Indian Ripple Road, Dayton, Ohio 45440**
****Air Force Research Lab, Dayton, Ohio**

Keywords: *Pressure-Sensitive Paint, Stereo Photogrammetry*

ABSTRACT

The assessment of advanced technology in the United States Air Force is becoming more reliant on the accuracy and fidelity of numerical predictions. It is expedient therefore, to validate the numerical codes upon which these assessments are based. The validation process requires the direct comparison of experimental measurements and numerical predictions. Among the issues that hinder the comparison of experimental measurements and computational predictions is the accuracy and structural integrity of the physical model. The computations are performed on a perfect model while the physical model includes imperfections and deforms under aerodynamic loading. The ability to monitor the structural deformation of the model while simultaneously acquiring experimental data is desirable. In an effort to resolve this issue, an experimental system that integrates Binary Pressure-Sensitive Paint and Stereo Photogrammetry into a single system has been developed. Stereo Photogrammetry utilizes two images of the model to provide quantitative measurements of the displacement and deformation of the model surface. Pressure-Sensitive Paint allows non-intrusive measurements of pressure with high spatial resolution. Binary-Pressure Sensitive Paint uses a reference channel to compensate for errors that result from variations in temperature and illumination over the model surface. In fact, the deformation of the model is a major source of error for traditional Pressure-Sensitive Paint measurements. An added advantage of binary pressure-sensitive paint is the elimination of all but a single wind-off measurement, thus increasing tunnel productivity. Image based techniques for making deformation measurements on aerodynamic models while using Pressure-Sensitive Paint have been demonstrated; however, this system integrates the measurement of pressure and deformation into a single system. Experimental measurements of pressure and deformation using the integrated system have been conducted on an Unmanned Combat Air Vehicle model in the Subsonic Aerodynamics Research Laboratory wind tunnel at Wright-Patterson Air Force Base. The Pressure-Sensitive Paint results are compared to traditional pressure taps. Deformation results are also compared to predictions from a computational model.

1 INTRODUCTION

While measurements of pressure using Pressure-Sensitive Paint [1] (PSP) have been demonstrated in high-speed wind tunnels, several issues that limit the accuracy of the technique [2] have been identified. Among these issues are errors due to displacement and deformation of the wind tunnel model, instability of the illumination source, photo-degradation and sedimentation of the painted surface, and non-uniform temperatures on the model surface. Errors in PSP measurements have prevented wide deployment of PSP systems for commercial applications. An approach that

minimizes these errors in PSP measurements would provide a significant benefit for research and could result in wider commercial acceptance of the PSP technique.

Measurements of model deformation using image based techniques have been successfully demonstrated by several teams [3, 4, 5]. The direct measurement of model geometry has several benefits. Utilization of image based measurements of pressure requires that the two-dimensional image be mapped onto the three-dimensional geometry for comparison to computational models. Furthermore, the direct measurement of the experimental geometry is of significant value when comparing theoretical or computational results to actual experimental measurements. Combined measurements of pressure using PSP and geometry have been demonstrated however, these measurements were accomplished using independent systems. A single system capable of performing simultaneous measurements of pressure and model geometry would be of significant value. Such a system should lower the overall cost of each technique and improve tunnel productivity. The goal of the current work is to combine measurements of pressure and model geometry into a single system.

2 PRESSURE-SENSITIVE PAINT

A typical pressure sensitive paint is composed of two main parts, an oxygen-sensitive fluorescent molecule, and an oxygen permeable binder. The pressure sensitive paint method is based on the sensitivity of certain luminescent molecules to the presence of oxygen. When a luminescent molecule absorbs a photon, it transitions to an excited singlet energy state. The molecule then typically recovers to the ground state by the emission of a photon of a longer wavelength. In some materials oxygen can interact with the molecule such that the transition to the ground state is nonradiative, this process is known as oxygen quenching. The rate at which these two processes compete is dependent on the partial pressure of oxygen present, with a higher oxygen pressure quenching the molecule more, thus giving off a lower intensity of light.

Image based pressure measurements using PSP are accomplished by coating the model surface with the paint and illuminating the surface with light of the appropriate wavelength to excite the luminescent molecule. The surface is imaged through a long-pass filter to separate the luminescent signal from the excitation light and the luminescent signal distribution is recorded. Unfortunately, the luminescent signal from the paint is not only a function of pressure. The luminescence varies with illumination intensity, probe concentration, paint layer thickness, and detector sensitivity. These spatial variations result in a non-uniform luminescent signal from the painted surface. The spatial variations are eliminated by taking the ratio of the luminescent intensity of the paint at an unknown test condition, I , with the luminescent intensity of the paint at a known reference condition, I_o . Using this *wind-on wind-off* ratio, the response of the system can be modeled using a modification of the Stern-Volmer equation.

$$\frac{I_o}{I} = A(T) + B(T) \frac{P}{P_o} \quad (1)$$

3 ERRORS IN PSP MEASUREMENTS

Sources of uncertainty for PSP measurements have been investigated and modeled by Liu [2]. These error sources include temperature, illumination, model displacement/deformation, sedimentation, photo-degradation, and camera shot noise. Liu concluded that the major sources of error were temperature and illumination. These two sources of error will be discussed and the

minimization of these errors through the use of Binary PSP will be discussed. Errors due to temperature will be considered first.

Note in equation 1 that the Stern-Volmer coefficients, $A(T)$ and $B(T)$ are functions of temperature. The Stern-Volmer coefficients are temperature dependent because temperature affects both nonradiative deactivation and oxygen diffusion in a polymer. In fact, the temperature dependence of $A(T)$ is due to thermal quenching while the temperature dependence of $B(T)$ is related to the diffusivity of oxygen in a polymer binder. Temperature sensitivity can lead to errors in converting the intensity distributions to pressure. This is demonstrated by considering a calibration of a PSP composed of Platinum Tetra(pentafluorophenyl)porphine (PtTFPP) in Fluoro/Isopropyl/Butyl (FIB), which has a temperature sensitivity of 0.5% per degree K. The quantity I_o/I is a monotonic function of pressure along any isotherm. The *wind-on* and *wind-off* images however, must be acquired at the same temperature if the conversion to pressure is to free from temperature errors. A second temperature related issue is the slope of the curve along each isotherm. For most PSP's, the slope of the sensitivity curve is a function of temperature. An accurate measurement of the absolute temperature is necessary to correctly convert the intensity ratio to pressure. An important property of the PtTFPP/FIB paint is the property of ideality [6]. For an ideal paint, the slope of the sensitivity curve is independent of temperature. This property is of significant value for minimizing temperature errors in PSP measurements. It is also a significant advantage in the production of a temperature compensating Binary PSP.

For radiometric PSP, errors in pressure measurements due to temperature are largely the result of changes in the temperature of the model surface between the acquisition of the *wind-off* and *wind-on* image. However, any temperature gradient on the model surface will still result in a temperature-induced error in the pressure measurements. These temperature gradients can be the result of model construction, tunnel operation, or fluid dynamics. The UCAV model is constructed using an internal metal structure and a polymer resin. The thermal signature of the internal structure is apparent when the surface of the model is subjected to a heat flux. The model is commonly exposed to a heat flux due to changes in tunnel Mach number. This condition is most apparent during tunnel startup. While the model will eventually reach equilibrium with the tunnel, productivity requires that data acquisition continue and elimination of temperature errors will provide a significant increase in data accuracy under these conditions. Even after the model has reached thermal equilibrium the temperature distribution on the model is not necessarily uniform. One example of a temperature gradient generated by the external flow is boundary layer transition. In this case, one must consider the recovery temperature and the state of the boundary layer. Assuming a Mach number of 0.4, boundary layer transition should result in a temperature gradient of about 0.5 degrees Kelvin. The UCAV model is constructed from a low thermal conductivity material therefore the boundary condition is close to adiabatic. The temperature gradient will be close to the 0.5 Kelvin but the model surface will reach a steady state temperature quickly. Assuming the temperature sensitivity of PTFPP/FIB, this temperature gradient will produce an error in pressure of about 0.1 psi.

The relationship between surface illumination and paint luminescence is linear; therefore, any change in surface illumination will result in an equal change in paint luminescence. Errors in pressure measurements caused by variations in surface illumination can stem from several sources as discussed by Liu [2]. These sources include deformation of the model surface, physical displacement of the model or illumination source, and temporal instability in the illumination source. Regardless of the source, any variation of the illumination intensity at the painted surface of the between the *wind-off* and *wind-on* images will register as an error in illumination.

4 BINARY PRESSURE-SENSITIVE PAINT

One means of dealing with the issue of illumination errors is to employ a reference probe as shown in Figure 1. In fact, several groups have successfully demonstrated this approach [7, 8]. The goal is to use the luminescence of the reference probe to correct for variations in the luminescence of the signal probe (the pressure sensor) that are caused by variations in illumination. This is accomplished by taking a ratio of the luminescence of the signal probe to the luminescence of the reference probe. Assuming that both the signal and probes response is linearly proportional to the local illumination and probe number density the resulting function is:

$$R(P, T, n_S, n_R) = \frac{F_S(P, T) n_S I}{F_R(P, T) n_R I} \quad (2)$$

The dependence of R on illumination has been removed; however R is still a function of temperature, pressure, and the concentration of each probe. If the distributions of the signal and reference probes are identical, the dependence on probe concentration is removed. This condition however, is difficult to achieve. To eliminate the effects of probe concentration, the standard *wind on* and *wind off* ratio (a ratio of ratios) is applied.

$$S(P, T) = \frac{R_0(P_0, T_0) n_S / n_R}{R(P, T) n_S / n_R} = \frac{R_0(P_0, T_0)}{R(P, T)} \quad (3)$$

The system response S is now a function of pressure and temperature only. At first glance, this ratio of ratios procedure may not seem to be an improvement over the standard radiometric approach. However, the relative concentration of each probe is static therefore only a single *wind-off* is needed. This is a significant improvement in tunnel productivity as it reduces the number of test conditions by a factor of two.

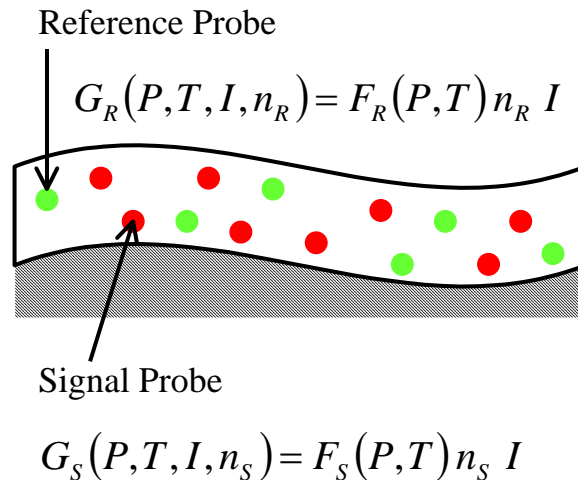


Figure 1 Binary Pressure-Sensitive Paint.

With illumination removed from equation 3, the goal becomes minimizing the sensitivity of the system to temperature. The approach utilized involves allowing the reference probe, which is

eliminating sensitivity to illumination, to compensate for the temperature sensitivity as well. This is accomplished by adding two constraints to the selection criteria already outlined for a self-referencing paint. 1) The combination of the signal probe and paint binder must form an ideal paint and 2) the temperature sensitivity of the reference probe must match the temperature sensitivity of the ideal paint. A PSP composed of PtTFPP/FIB is a good candidate for a binary paint. PtTFPP/FIB is an ideal paint with low temperature sensitivity. A binary PSP composed of PtTFPP/FIB and a selected reference probe has been used to produce a PSP system with little temperature sensitivity. The calibration of this paint is has a temperature sensitivity of less than 0.05% per degree K over a range of temperatures from 5 – 45 C and pressures from 1 – 20 psia.

5 STEREO PHOTOGRAMMETRY

Image based measurements in wind tunnels have been used to determine quantities such as model deformation [4] and angle of attack. It is desirable to combine measurements of pressure using PSP with model geometry to facilitate comparison of experimental and computational results. PSP may be implemented as an imaged-based technique. Obtaining three-dimensional information from plane images is accomplished using the principals of photogrammetry. It is noted that measurements of pressure using PSP and model geometry using photogrammetry have been demonstrated. These measurements however, were accomplished using independent systems. In general, the information necessary for determining model geometry is contained within the PSP images. By applying photogrammetry principals to PSP images, a system has been developed for acquiring pressure and model geometry using the same images.

In general, the model geometry may be determined using a single image. Some simplification of the process is obtained by acquiring two views of the model. Binary PSP requires two images of the model, a signal and reference image. While it is common to acquire these images using a single camera and a filter switch, two independent views of the model are also acceptable. The latter approach is used in developing the combined Binary PSP Stereo Photogrammetry system.

General photogrammetry often requires a complex calibration process. A point at real world location (X_w, Y_w, Z_w) is projected onto the image plane of the camera at (X, Y) . If the exact position and orientation of each camera is known, the real world position of the point can be determined from trigonometry relationships. However, precisely measuring the orientation and location of the cameras can be difficult. The method of photogrammetry instead uses a generalized matrix model to form a map from the camera image planes back to the real world coordinate system.

Calibration points are used to provide known locations in real space that correspond to certain known locations in the camera image planes. The cameras must all contain the calibration points within their field of view. For each calibration point with real world position $(X_w, Y_w, Z_w)_n$, each camera sees the point on its image plane at a unique location $(X, Y)_n$. This transformation can be described by functions:

$$\begin{aligned} (X, Y)_n &= f_n(X_w, Y_w, Z_w, a_1, \dots, a_N) \\ n &= 1, 2, \dots, N \end{aligned} \tag{4}$$

Through the use of calibration points, the coefficients a_n can be determined. For the purposes of PSP, the model geometry is well defined and the displacements are small compared to the scale of the model. These conditions provide creation of linear system of equations connecting displacements in image plane $(\Delta X, \Delta Y)_n$ with model deformations $(\Delta X_w, \Delta Y_w, \Delta Z_w)$ in the calibration points:

$$\begin{aligned}
 (\Delta X, \Delta Y)_n &= f_{nx} \Delta X_w + f_{ny} \Delta Y_w + f_{nz} \Delta Z_w \\
 n &= 1, 2, \dots, N \\
 f_{nx} &\text{ is partial derivative in } (X_w, Y_w, Z_w)
 \end{aligned}
 \tag{5}$$

For a data set that uses two cameras, this system is over-determined and the linear system can be solved.

A schematic of the combined system is shown in Figure 2. The signal camera is placed near the nose of the model and the reference camera is placed near the tail providing a stereo view of the model. The pressure taps act as markers for the system for both the PSP resection process and for tracking model deformation. The location of the pressure taps on the model is well defined in the model geometry. The markers are located on the image bitmaps (X,Y) of each image and these bitmap coordinates are converted to physical space (X_w, Y_w, Z_w) using the calibration. The system is calibrated by acquiring images of the model at several angles of attack. The locations of the markers were measured using a Coordinate Measurement Machine (CMM). These marker locations were used in the camera calibration process.

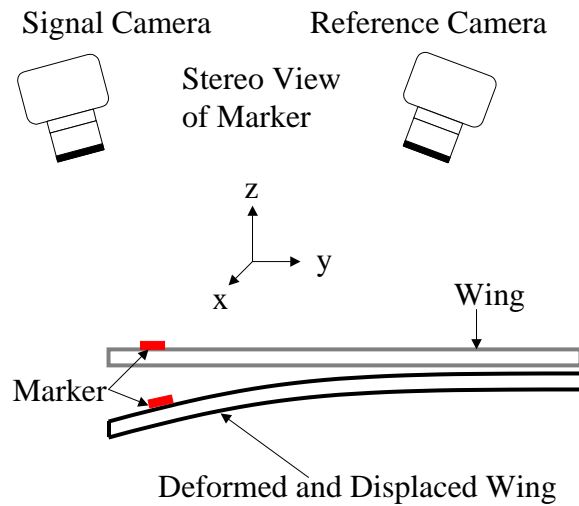


Figure 2 Stereo Model Deformation System.

6 EXPERIMENTAL SETUP

The UCAV experiments were performed in the SARL wind tunnel at Wright-Patterson Air Force Base. The SARL is an open-circuit, low-speed wind tunnel with a 3.05 meter by 2.13 meter test section and a maximum Mach number of 0.5. The tunnel provides excellent optical access with Pyrex windows on both the top and each side of the test section. The Boeing UCAV model, shown in Figure 3, is a hybrid design built by John Hopkins University Applied Physics Laboratory. The model is composed of an internal metal structure to withstand the aerodynamic loading and an external geometry constructed using a rapid-prototype stereo-lithography polymer. The model has a lambda wing with a span of approximately 4 feet and length of 3 feet. Control surfaces on the trailing edge were adjusted to -20, 0, and +20 degrees for the current tests. The angle of attach was varied from 12 to 20 degrees and measurements were conducted at Mach numbers of 0.2 and 0.4.

SIMULTANIOUS MEASUREMENTS OF PRESSURE AND DEFORMATION ON A UCAV IN THE SARL

The UCAV model was provided by Dr. Charles Tyler who conducted both computational (second order three-dimensional Euler simulation) and traditional experimental studies (i.e. aerodynamic force and moments, pressure taps) of the flow field associated with this model. Results from the PSP and SP experiments are to be compared to these experimental and computational results. Again, the goal of this program is to develop new experimental tools for rapid evaluation of aerodynamic designs and validation of CFD predictions.

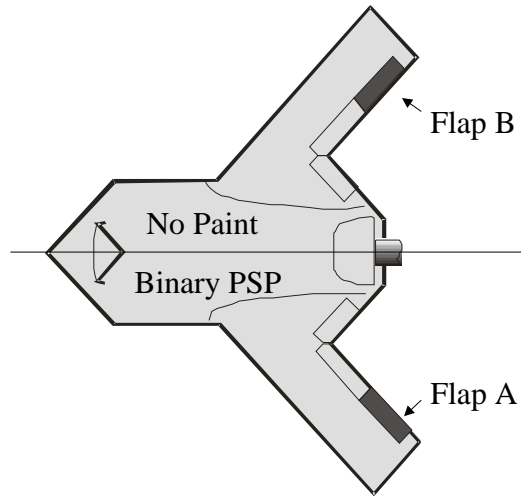


Figure 3 Boeing UCAV Model.

The first goal of this experimental campaign was to demonstrate Binary PSP in the SARL. Demonstration of simultaneous PSP and deformation measurements was a secondary goal for this entry. For these reasons, two experimental setups were employed; one specifically for acquiring PSP measurements on the entire UCAV model, and one for demonstrating PSP and deformation measurements on the UCAV wing.

For demonstration of Binary PSP measurements the setup included two PixelVision SpectraVideo cameras. The SpectraVideo is a cooled, back-illuminated CCD with a full-well capacity of 300,000 photo-electrons and a 16-bit readout. One camera viewed the front half of the model while the second camera viewed the back half. Each camera was combined with a 50mm f/4 Nikon lens and an ISSI FSW-2 filter switch. The filter switch holds up to four, 2 inch filters in front of the camera lens. The filter switch communicates with the data acquisition program through an RS-485 interface. The camera and filter switch are mounted onto an optical rail to form a single unit and this rail is mounted onto a rotation and tilt stage to expedite image alignment. Paint illumination is provided by four ISSI-LM4 LED arrays. The LM-4 provides ~ 1.6 W of illumination at 405 nm. To facilitate data acquisition while alternating data images and background images the arrays were operated in Long-Pulse mode. In Long-Pulse mode, the array is controlled by a TTL pulse; the array however, is not over-driven. This allows the exposure time to be varied between 10 μ s and DC operation. In Long-Pulse mode, the output of the arrays does not reach the steady state stability of the standard LM-4 LED; however, for the use of Binary PSP only pulse to pulse repeatability is an issue. All data acquisition procedures are controlled using a single PC and GUI based data acquisition program. The program is used to control two cameras, two filter switches, and a DG-535 using a single computer. The program communicates with the cameras using two Lynx serial cards

and the filter switches are controlled using an RS-485 interface. The DG-535 pulse generator is controlled over a GPIB interface and is used to control the LED arrays.

The demonstration of simultaneous PSP and deformation measurements employed the same data acquisition system. In this case however, the view of each camera was repositioned to include the wing of the UCAV model. In this case, the calibration process included setting the model to angles of attack of 12 degrees and 20 degrees. Images of the wing were acquired at these conditions and a CMM was used to locate the positions of the pressure taps at each angle of attack. The pressure taps served as markers for both the PSP resection process and for the model deformation measurements. Data acquisition again included a set of wind-off and wind-on images through each filter. This data was processed to determine pressure in a manner identical to the preceding discussion. To determine model deflection and deformation, the position of the pressure taps on the bitmaps were determined and converted to world coordinates using the calibration. This data set represents a discrete set of information. These data points were used as the basis of an interpolation procedure to produce a continuous map of wing deflection.

7 DATA ACQUISITION PROCEDURE

One source of noise for PSP measurements that has been an issue in past SARL tests is background noise. The SARL is an open circuit tunnel and therefore, it is difficult to eliminate ambient light. In general, some level of background lighting is always present for PSP tests. This issue is usually resolved by acquiring an image of the test article with the illumination off. This background is then subtracted from the data images to remove the background noise. This procedure assumes that the background lighting is constant; this is not the case in the SARL. The background varies from about 1% to 30% of the dynamic range of the camera during the day. Furthermore, this background can change substantially in a short time due to cloud cover. To minimize this dynamic background effect, a background image was acquired on every fifth exposure. These wind-on backgrounds are then used to minimize the error due to background lighting.

Just as with radiometric PSP, data is acquired at wind-on and wind-off conditions however, at each condition data must be acquired through two filters. This is accomplished using the filter switch. A second modification in the procedure is the number of wind-off conditions that must be acquired. The use of a Binary PSP eliminates the need for wind-off images at each condition. This can significantly increase tunnel productivity as it eliminates a significant number of wind-off conditions. Data acquisition is begun by setting the model at an angle of attack of 12 degrees and a set of data images is acquired. Each data set includes one background and four data shots through each filter for a total of ten images. This set completes the wind-off acquisition. The tunnel is started and a data set, including backgrounds, is acquired at each test condition. The images at each condition are averaged and the background is subtracted. Preliminary filtering is applied to each image and the ratio of the signal to reference image is computed. The wind-off and wind-on ratio images are then mapped onto the mesh of the UCAV model and the remaining data processing for conversion to pressure is accomplished on the mesh.

8 RESULTS

The pressure distribution for the UCAV model at Mach 0.2 and Mach 0.4 at 20 degrees angle of attack is shown in Figure 4. The defining aerodynamic features are evident in this image. A strong vortex that originates at the nose of the model propagates along the leading edge of the model. This vortex eventually bursts and propagates along the side of the model. The pressure signature of this vortex on the side of the model surface is weak. This indicates that the vortex has burst or is no

SIMULTANIOUS MEASUREMENTS OF PRESSURE AND DEFORMATION ON A UCAV IN THE SARL

longer moving along the side of the model. The presence of the vortex is clearly visible in the velocity field as shown in Figure 5. This data indicates that the vortex is present near the side of the model but the low stream-wise velocity in the core indicates that the vortex has burst. Near the wing/body junction, a secondary vortex appears on the wing and sweeps outboard along the wing. This strong secondary vortex is also evident in Figure 5. After a short distance, the pressure signature of this vortex abruptly diminishes but continues to move along the span of the wing. Again, some insight into this behavior is gained by considering the velocity field. As this vortex sweeps along the wing, it is positioned very close to the surface. This will enhance the pressure signature of the vortex on the surface. The lower pressure could be due to the vortex lifting off of the wing or from a bursting of the vortex. The velocity data at a plane 6.5 inches downstream of the wing/body junction, also shown in Figure 5, indicates that the vortex has burst.

As the Mach number is increased to 0.4, the basic features of the flow remain unchanged as shown by the pressure distribution in Figure 4. The magnitude of the pressures increases with the square of velocity, therefore the features are more pronounced.

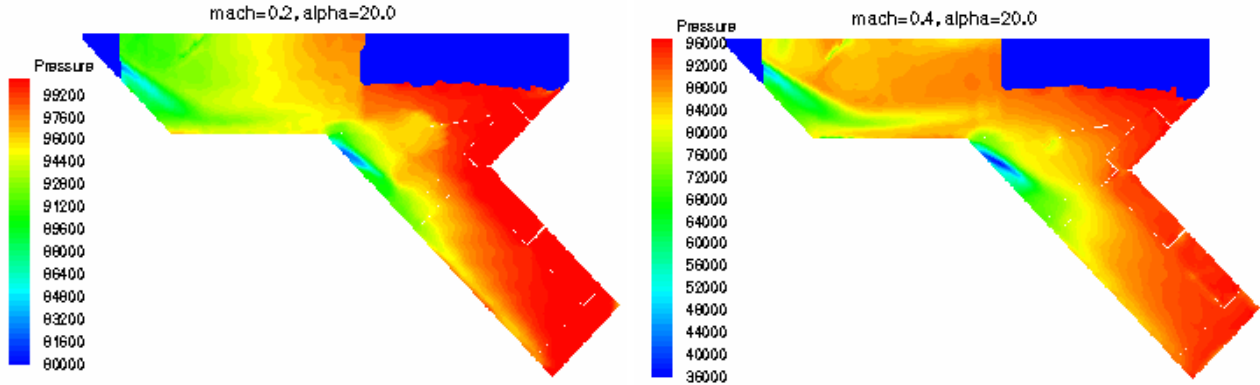


Figure 4 Pressure distribution on UCAV at Mach 0.2 and 0.4, at 20 degree angle of attack, and flaps at 0 degrees.

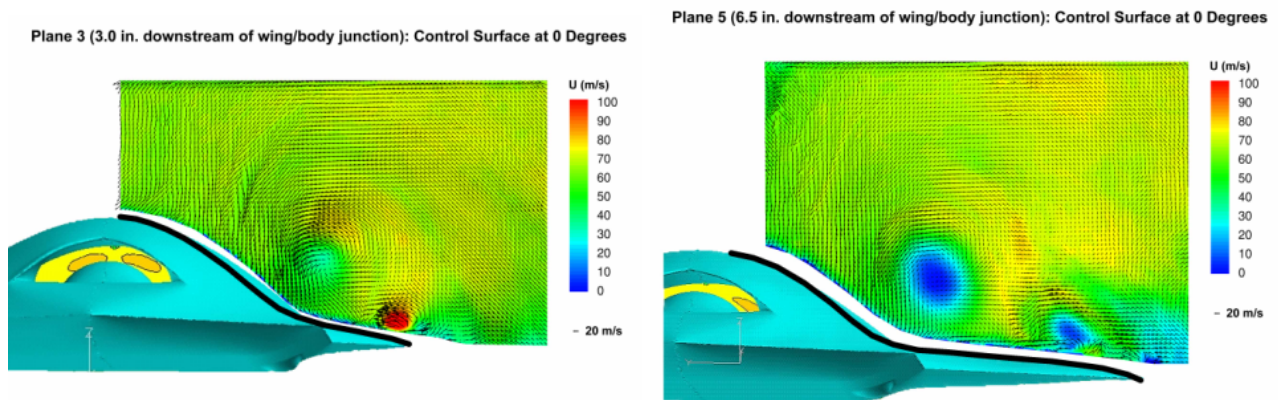


Figure 5 Velocity field of the UCAV at two planes at Mach 0.2 and 20 degree angle of attack with flaps at 0 degrees.

An estimate of the accuracy of the PSP measurements is obtained by plotting the pressure from the PSP near the taps versus the tap pressure. This data was compiled at over 40 tap locations. The mean squared deviation in this plot is about 700 Pa (0.1 psi); this deviation is substantially larger

than that obtained by Bell using the same PSP. In this case, the major source of error is believed to be background illumination. For this test, only four 4-inch LED lamps were available. This level of illumination required longer exposure times and therefore, higher levels of background noise. While the interlaced backgrounds improved the signal to noise ratio by mitigating the effects of the variable background, some error remains. To minimize this problem on future tests, more lamps are required to increase the signal level and improve the signal to noise ratio. Mitigation of the influence of the background noise can be improved by alternating background and data images.

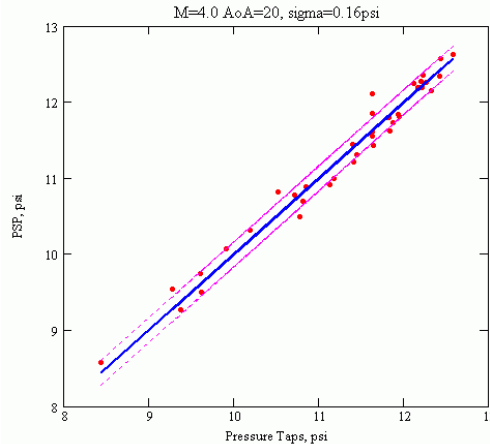


Figure 6 PSP measurement versus conventional tap pressure at 40 locations on the UCAV model.

Deformation measurements were demonstrated on a single configuration. The deformation of the model at 20 degrees angle of attack and Mach 0.4 is shown in Figure 7. These measurements indicate both a bulk shift of the model and bending of the wing. The bulk shift is approximately 0.6 inches at the spine of the model near the wing/body junction. The bending of the wing from the body to the tip is about 0.4 inches for this test condition. The bulk shift of the model can be a significant source of error for standard PSP. The wing bending of 0.4 inches is close to the value predicted for this model prior to the test. It is noted that the pseudo-continuous results presented here are the result of deformation measurements at a series of discrete points on the model. The data from these discrete points was interpolated to generate the continuous distribution shown here. While some aerodynamic models have been shown to have compound deformations [5], higher order bending is unlikely for this model.

9 CONCLUSIONS

A system capable of simultaneous pressure and deformation measurements has been developed. This system integrates Binary Pressure-Sensitive Paint and Stereo Photogrammetry into a single system. Binary Pressure-Sensitive Paint provides PSP measurements that are compensated for errors from temperature and illumination. Stereo Photogrammetry utilizes two images of the model to provide quantitative measurements of the displacement and deformation of the model surface. Experimental measurements of pressure and deformation using the integrated system have been conducted on an Unmanned Combat Air Vehicle model in the Subsonic Aerodynamics Research Laboratory wind tunnel at Wright-Patterson Air Force Base. The mean squared deviation between the Pressure-Sensitive Paint results and the pressure taps was ~ 0.1 psi. Deformation measurements indicate a bulk displacement of the model as well as bending of the wing under aerodynamic load.

SIMULTANIOUS MEASUREMENTS OF PRESSURE AND DEFORMATION ON A UCAV IN THE SARL

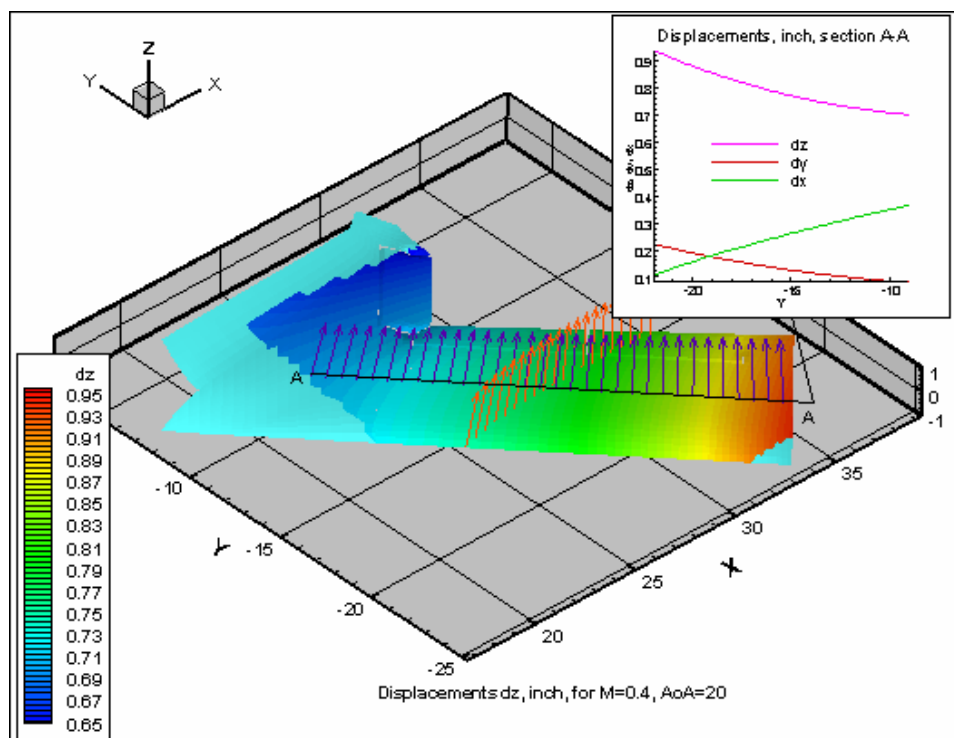


Figure 7 Displacement and Deformation of the UCAV model at 20 degree angle of attack and Mach 0.4.

10 ACKNOWLEDGMENTS

The authors would like to thank Prof. Gregg Elliott, Dr. Cam Carter, Dr Hank Baust, and Dr. Tom Beutner for their efforts in obtaining the Planar Doppler Velocimetry data.

11 REFERENCES

1. Liu T, Campbell B, Burns S, Sullivan J. Temperature and Pressure-Sensitive Paints in Aerodynamics. *Applied Mechanics Reviews*, Vol. 50, No. 4, pp. 227-246
2. Liu T, Guille M, Sullivan J. Accuracy of Pressure Sensitive Paint. *AIAA Journal*, Vol. 39, No. 1
3. Bell J, McLachlan, B, Image Registration for Pressure-Sensitive Paint Applications. *Experiments in Fluids*, Vol. 22, No. 1, pp. 78-86
4. Liu T, Cattafesta L, Radeztsky R, Burner A, Photogrammetry Applied to Wind-Tunnel Testing. *AIAA Journal*, Vol. 38, No. 6, pp. 964-971
5. Fleming G, Gorton S, Measurements of rotorcraft blade deformation using Projection Moire Interferometry. *Journal of Shock and Vibration*, Vol. 7, No. 3
6. Puklin E, Carlson B, Gouin S, Costin C, Green E, Ponomarev S, Tanji H, Gouterman M, Ideality of Pressure-Sensitive Paint. I. Platinum Tetra(pentafluorophenyl)porphine in Fluoroacrylic Polymer. *Journal of Applied Polymer Science*, Vol. 77, pp. 2795-2804
7. Bykov A, Fonov S, Mosharov V, Orlov A, Pesetsky V, Radchenko V. Study Result for the Application of Two-component PSP Technology to Aerodynamic Experiment. *AGARD'97*
8. Khalil G, Costin C, Crafton J, Jones E, Grenoble S, Gouterman M, Callis J, Dalton L. Dual Luminophor Pressure Sensitive Paint I: Ratio of Reference to Sensor Giving a Small Temperature Dependence. *Sensors and Actuators B*, Vol. 97, No. 1, pp. 13-21